Optical Kerr effect of liquid water: a new insight into the vibrational and structural dynamics

A. Taschin[1], P. Bartolini[1], R. Eramo[1,2], R. Righini [1,3], and R. Torre[1,4]

[1]*European lab. for Non-Linear Spectroscopy (LENS), Univ. di Firenze, via N. Carrara 1, I-50019 Sesto Fiorentino, Firenze, Italy.*

[2]*Istituto Nazionale Ottica, CNR, Largo Fermi 6, I-50125 Firenze, Italy.*

[3]*Dip. di Chimica, Univ. di Firenze, via Della Lastruccia 13, I-50019 Sesto Fiorentino, Firenze, Italy.*

[4]*Dip. di Fisica e Astronomia, Univ. di Firenze, via Sansone 1, I-50019 Sesto Fiorentino, Firenze, Italy.*

(Dated: April 11, 2013)

Abstract

The liquid and supercooled states of water show a series of anomalies whose nature is lively debated. A key role is attributed to the formation of structural aggregations induced by critical phenomena occurring deep in the supercooled region, not experimentally accessible for bulk water. This explain why, despite the numerous experimental investigations, the nature of water anomalies and the hidden critical processes remain elusive. Here we present a time-resolved optical Kerr effect investigation of the vibrational and relaxation processes in supercooled bulk water. The experiment measures the water intermolecular vibrations and the structural relaxation process in an extended temperature range, and with unpreceded data quality. A mode-coupling analysis of the experimental data allows the characterization of the intermolecular vibrational modes and of their interplay with the structural relaxation process.

I. INTRODUCTION

Water can remain liquid below its melting point and stays in its metastable phase known as supercooled water [1, 2]. Several thermodynamic (e.g. isothermal compressibility, isobaric heat capacity and thermal expansion coefficient) and dynamic (e.g. viscosity, diffusivity, structural relaxation) observables of liquid water show an anomalous behaviour [5]. In the supercooled state the values of these physical observables clearly diverge, with a singularity temperature T_s estimated at $\simeq 228$ K. Despite the wide interest and the numerous research efforts on this subject, the origin of these critical phenomena remained unclear [6–8] and lively debated [4, 9–15].

It is widely accepted that the water anomalies are connected with the formation of various structural aggregates whose features are modified by the temperature/pressure conditions [5]. A crucial point is the physical origin of these structural aggregations.

In their pioneering work Poole, Sciortino, Essmann, and Stanley [3] postulated the existence of a liquid-liquid critical point (LLCP), based on a simulation study and on the experimental observation of polyamorphism in glassy water (i.e. the existence of two forms of water glass: low-density and high-density amorphous ice). In the LLCP hypothesis a first order phase transition take places involving two supercooled water liquid forms: the low-density and the high-density phases. The low-density phase is characterized by tetrahedral intermolecular coordination, while the high-density one shows more packed structures with distorted networks. The existence of a LLCP is compatible with a series of computational and experimental results [5]. Recent new simulation studies confirmed the LLCP hyphotesis [4, 12–15]. Nevertheless, the matter is still under debate: in their recent simulation study, Limmer and Chandler interpreted the water anomalies as non-equilibrium phenomena associated to the liquid-crystal transition [11]. Moreover the relevance of ice nucleation phenomena and their relationship with the water anomalies has been reported [9, 10].

A fundamental question in order to explain the origin of water anomalies is if these two liquid forms persist at temperature higher than T_s, where they must be considered as local and transient structures. The fluctuations between the two water species could explain the thermodynamic and dynamic anomalies. Unfortunately, the most evident critical phenomena are expected to occur in the supercooled phase at temperature/pressure values not directly accessible in bulk water samples, and this prevents a direct experimental solution

of the problem. In fact, in several experimental and simulation works the water singularity temperature T_s at atmospheric pressure has been extrapolated to be around 223-228 K, while homogeneous nucleation fixes the lowest reachable temperature at about 231 K for liquid water. Actually, in a macroscopic bulk sample the crystallization phenomena and several experimental difficulties limit the minimum temperature around 243 K. Nano-confinement has the advantage of preventing water freezing and of extending the experimental investigation of the supercooled phase down to very low temperatures; it is however still unclear to what extent the interactions with the pore surfaces modify the water properties [16–19]. The hydrogen bond network largely determines the intra- and inter-molecular vibrational spectrum of supercooled water; thus the experimental investigation of the spectral features gives precious information on the local intermolecular structures and on their variation with the temperature/pressure conditions. The investigation of high frequency spectrum, 1000-4000 cm^{-1}, gives access to the intra-molecular vibrational dynamics. In a recent paper Mallamace et al. [20] investigated the OH vibrational spectra of confined supercooled water by means of Fourier transform infra-red spectroscopy (FTIR). According to their experimental results a new vibrational component at 3120 cm^{-1} appears at low temperature, whose intensity increases sharply in the deep supercooled phase. The authors attribute this component to the low-density water liquid form. The low frequency spectrum of water, $\nu < 1000$ cm^{-1}, reflects the inter-molecular dynamics and so it is particularly sensitive to the local molecular structures. This frequency range of the water spectrum has been investigated in several light scattering studies, see for example [21–27]. Two main broad peaks are observed at 50 and 200 cm^{-1}, generally attributed to the hydrogen bond "stretching" and "bending" vibrations. The spectra show also a very low frequency wing, $\nu < 20$ cm^{-1}, that has been attributed to "relaxation" processes. The light scattering data were measured at relatively high temperatures and have rather poor signal-to-noise ratio, due to the very weak water signal: these drawbacks did not allow identifying all the possible vibrational modes possibly contributing to the water spectrum in this region. Moreover, the reported attempts of fitting the light scattering data have been based on a simple superposition of independent Gaussian and Lorentzian functions, neglecting any possible coupling between the vibrational dynamics and the structural relaxation processes.

An accurate analysis of the low frequency spectral features of supercooled water, including a quantitative comparison to the predictions of recent models for water dynamics is

still missing; it actually appears as a required step towards the full understanding of the structural and dynamical properties of water in its low temperature metastable state.

In recent years, time-resolved non-linear spectroscopy demonstrated to be a very useful tool for the investigation of complex liquid dynamics [28]. Several studies of this type have been performed on liquid water; only in few cases they have been extended to its supercooled phase [29–32]. Time-resolved optical Kerr effect (OKE) investigations of liquid water [29, 33–36] show the signature of fast vibrational dynamics at short times, followed by a slower monotonic relaxation. The initial oscillatory component provides information about intermolecular hydrogen-bond dynamics, and can be directly compared with the low-frequency Raman spectrum [33]. Actually, the OKE experiments on supercooled water [29] have been focused so far on the investigation of the slower decay, which is interpreted as a structural relaxation phenomenon. No detailed OKE investigation of the vibrational dynamics in supercooled water has been carried out, due to the intrinsic experimental difficulties, so that a detailed picture of this dynamics is still missing [37]. Using an improved experimental set-up [31], we were able to measure, for the first time according to our knowledge, the fast vibrational dynamics and the slow structural relaxation in a single data set characterized by low noise and wide dynamic range. Moreover, we reached temperatures lower than in previous experiments, approaching the homogeneous nucleation limit. We succeeded in measuring the OKE signal relaxation over a large time interval of about 25 ps with a high time resolution of 20 fs. We can thus provide the unambiguous measurement of the entire correlation function in supercooled water, enabling a very stringent comparison with the available theoretical models.

II. EXPERIMENT AND METHODS

Time resolved optical Kerr effect (OKE) spectroscopy is a non-linear technique exploiting the transient birefringence induced by the electric field of radiation in an optically transparent and isotropic medium. The method has been described in many papers and review articles [28, 38–40]. In short, the oscillating electric field of a polarized short pulse of monochromatic light (the pump) induces optical birefringence in the sample. In addition to the instantaneous electronic contribution (which does not carry any dynamic information), the induced birefringence reflects the relaxation and vibrational response of the molecules in

the sample. A second pulse (the probe), spatially superimposed within the sample with the pump pulse and characterized by a different polarization, probes the induced birefringence. The intensity of probe light leaking through a polarizer placed after the sample measures the material response as a function of the time delay between pump and probe, the optical set-up is reported in the Supplementary Information. If femtosecond light pulses are employed, the method allows measuring the relaxation processes and the low frequency vibrational correlation functions of the system. In this sense it is the time-domain counterpart of depolarized light scattering technique [40]. The wide accessible time window, extending from tens of femtoseconds to hundreds of nanoseconds, makes OKE a very flexible technique, able of revealing very different dynamic regimes, from simple liquids to supercooled liquids and glass formers [29, 41–43]. In the case of optical heterodyne detection, the delay time dependent signal is directly proportional to the material response (relaxation) function, $R(t)$, convoluted with instrumental function, $G(t)$. The response $R(t)$ is directly connected to the time derivative of the time-dependent correlation function of the dielectric susceptibility [28, 39]

$$R(t) \propto \frac{\partial}{\partial t}\langle \chi(t)\chi(0)\rangle \tag{1}$$

The Fourier transform of $R(t)$ correspond to the frequency-dependent response, the observable measured in depolarized light scattering (DLS) experiments [28, 40]. We stress here that measuring the correct instrumental function $G(t)$ is a crucial step for achieving a reliable and accurate fitting of the experimental OKE signal. A detailed description of the method adopted is given in the supplementary information. In short, the critical point in the entire procedure is that any minor, apparently negligible adjustment of the optical set-up when passing from recording the instrumental function to measuring the water signal prevents the extraction of the real instrumental function. The resulting inaccurate deconvolution of the water signal degrades the quality of the overall fitting. In our experiments $G(t)$ was obtained by measuring the OKE signal of a CaF_2 plate placed in a purposely designed holder which allowed switching to the water sample without even touching the rest of optical set-up. Supercooling bulk water can be achieved only with particularly pure sample and using specific attention for the cooling procedure. We performed the measurements on a sealed vial of cylindrical shape, prepared for pharmaceutical purposes by the Angelini company, which allowed us to reach the temperature of 247 K. The sample temperature is controlled by means of home-made cryostat with a stability of 0.1 K, using a Peltier cooler. The laser

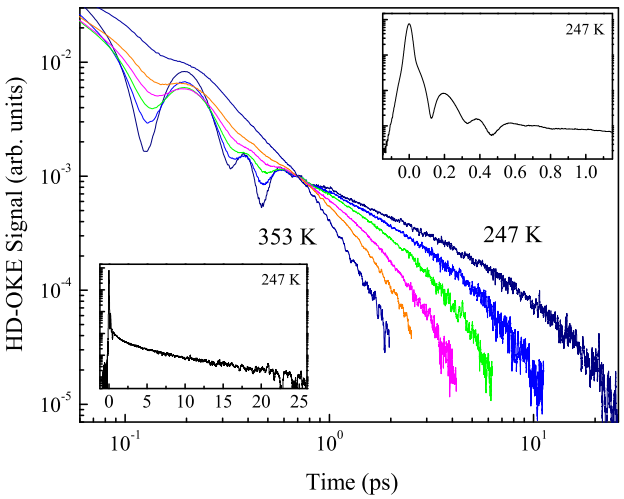

FIG. 1. HD-OKE signal as function of temperature in log-log plot. At short delay times (<1 ps), the HD-OKE signal shows oscillations due to vibrational dynamics, that become more defined as the temperature is lowered below the melting point. At longer delay times, the signal is characterised by a monotonous decay, that has a strong temperature dependence and a clear non-exponential nature. For a readable display, only 6 temperatures (247-258-273-293-313-353 K) out of the 11 measured (the previous ones plus 253-263-268-278-333 K) are reported; the intensities are normalized at 0.7 ps. The upper and lower insets show, in a log-linear plot, the 247 K HD-OKE data at short and long delay times, respectively.

system is a self-mode-locked Ti:sapphire laser producing pulse of 20 fs duration with an energy of 3 nJ [31]. The optical set-up and other details about the experimental apparatus are reported in the supplementary information.

III. RESULTS AND ANALYSIS

The heterodyne-detected OKE (HD-OKE) data are reported in Figure 1: the data clearly show the complex dynamic features presented by liquid and supercooled water. The vibrational dynamics, extending up to 1 psec, displays an articulate pattern that becomes progressively more defined going deep in the supercooled phase, and that at longer times merges into the monotonic decay due to structural relaxation. The time-resolved HD-OKE experiment measures the time-dependent correlation function of the collective water polar-

izability, see Equation (1). The time evolution of this function reflects the water dynamics thorough the electronic polarizability. Numerical investigations [37] show that the OKE signal of water, in all time scales, is the results of a complex interplay between intrinsic molecular terms and interaction-induced contributions. In particular, the fast oscillatory dynamics consists of a combination of collective hindered roto-translational motions.

The relaxation features presented by supercooled water are very similar to that of the glass-former liquids [43], and the slow dynamics is found in agreement with the main mode-coupling theory predictions [29]. In Fig.2 we report the master plot analysis of the slow component of the HD-OKE signal decay. The new data confirm, over an extended temperature range, the power law temperature dependence of the relaxation time. The analysis of the whole time-dependent correlation function measured by the optical experiments requires the utilization of a model that enables an operative parametrization of the vibrational modes present in the water dynamics. This turns out to be a complex task, and different attempts have been pursued [34–36] in that direction. None of these water studies was extended into the supercooled state. Moreover, the data analysis and fitting models adopted so far did not include any coupling between the fast vibrational dynamics and the slow structural relaxation. We tested some of these fitting procedures on our HD-OKE data and found that they fail to reproduce correctly the HD-OKE data in the supercooled temperature range. In order to analyze the vibrational dynamics and the structural relaxation including their coupling processes, we utilized the schematic solution of mode-coupling theory [44].

The formalism of mode-coupling theory (MC) stems from a generalization of the Mori and Zwanzig hydrodynamic theory [44]. In MC theory the retardation effects are taken into account by memory functions M(t), which play the role of the hydrodynamic friction coefficients. Of course the task of any microscopic theory is that of providing the form of M(t). In its simplest form, developed for simple atomic liquids, only density fluctuations contribute to memory; in order to overcome the limitations of this approach and to extend the MC theory description to the dynamics of more complex systems, several versions of the theory have been developed. For molecular liquids in fact orientational and intra-molecular degrees of freedom contribute to the overall dynamics. In our analysis we adopt the "schematic" formulation of the MC theory (SMC). Details of the theory are given in the supplementary. Briefly, in this approach the density-density time correlator, $\Phi_m \propto \langle \rho(t)\rho(0) \rangle$,termed the

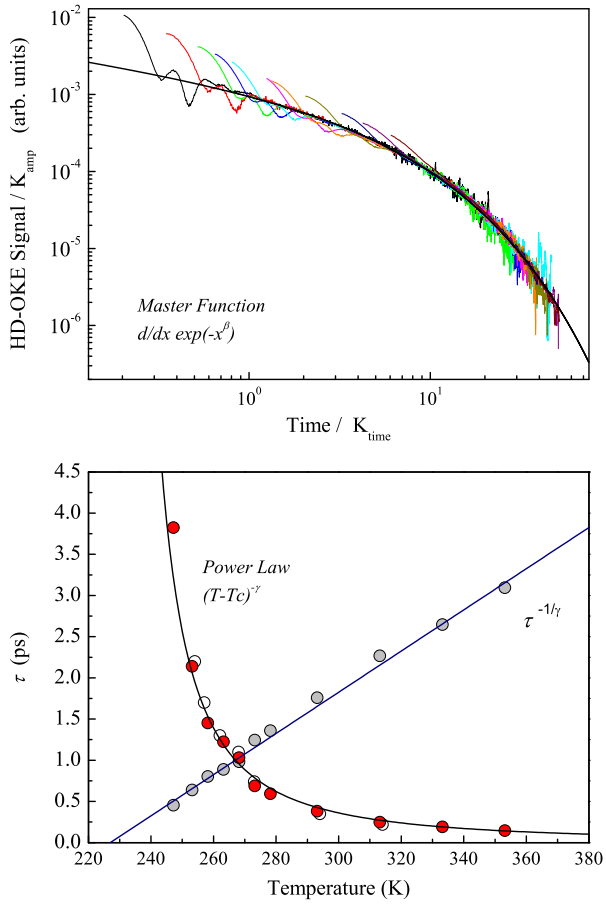

FIG. 2. The slow dynamics of supercooled water can be analyzed using a model-independent procedure [29], consisting in rescaling the time/amplitude scales of the raw data measured at different temperatures in a way that the decay curves overlap. If all the data collapse in a "master-plot", it is possible to identify a function, the "master function", that defines the relaxation independently of the temperature [44]. In the upper panel we report the master-plot of the HD-OKE data and the master function: $\frac{d}{dx}exp(-x^{\beta})$ with a stretching parameter $\beta = 0.6$. The relaxation times obtained with the rescaling procedure are shown in the lower panel of the figure. The new data (red circles) extend and confirm the previous data (empty circles) [29]. The temperature dependence of these data are in agreement with the power law: $\tau \propto (T - T_c)^{-\gamma}$, with a critical temperature $T_c \simeq 227$ K and a critical exponent $\gamma \simeq 1.7$. We report the relaxation times and the power law in a linearized plot, in order to visualize immediately the scaling proprieties and the critical temperature.

master correlator, is described by the differential equation:

$$\ddot{\Phi}_m(t) + \eta_m \dot{\Phi}_m(t) + \Omega_m^2 \Phi_m(t) + \int K(t-t')\dot{\Phi}_m(t')dt' = 0, \tag{2}$$

where Ω_m is the mode frequency, η_m is the shear viscosity and the memory function $K(t)$ is expressed as a series expansion of the master correlator itself. The role of other observables, A_i, linked to the density correlator dynamics (e.g. the molecular orientation, the dynamics of a target molecule, etc.) is described by a set of differential equations [39] of the same form as equation (2), written in terms of slave correlators $\Phi_i(t) \propto \langle A_i(t)A_i(0)\rangle$ and of memory functions of the form $m_i(t) = v_i^s \Phi_m(t)\Phi_i(t)$, which implies the coupling of the master and slave correlators. The key point in the SMC analysis of the OKE experimental data is that the time correlation function of the sample polarizability can be expressed as the sum of the time derivatives of the slave correlators:

$$R^{SMC}(t) \propto \frac{\partial}{\partial t} \sum_i \Phi_i(t). \tag{3}$$

We underline here that the individual slave correlators describe "average" collective modes, so that they cannot be associated to specific physical variables. In summary, the SMC approach represents a robust physical model able of describing a complex dynamics, with no need of unjustified assumptions concerning the decoupling of slow and fast dynamics.

We solved the SMC equations numerically, taking the frequencies, viscosities and coupling coefficients as parameters to be adjusted in order to reproduce the HD-OKE response by a fitting procedure.

The details on the SMC equations and fitting procedures are reported in the supplementary information. In Figure 3 we show some of the measured HD-OKE signals with the fits obtained using the SMC model. The model is able of reproducing correctly the experimental data over the whole time range at all temperatures. Most remarkably, and differently from other fitting models widely used, this result is achieved without imposing any non-physical decoupling of vibrational and relaxation dynamics. An important result of our work is that the fitting at temperatures $\leq$ 313 K requires three slave correlators, whereas for higher temperatures only two correlators are needed.

The time domain data, collected in the time-resolved HD-OKE experiments, are transformed to yield the corresponding spectra in the frequency domain. In fact,the Fourier transform of the HD-OKE response function, $\tilde{R}(\omega)$, is directly connected with the spec-

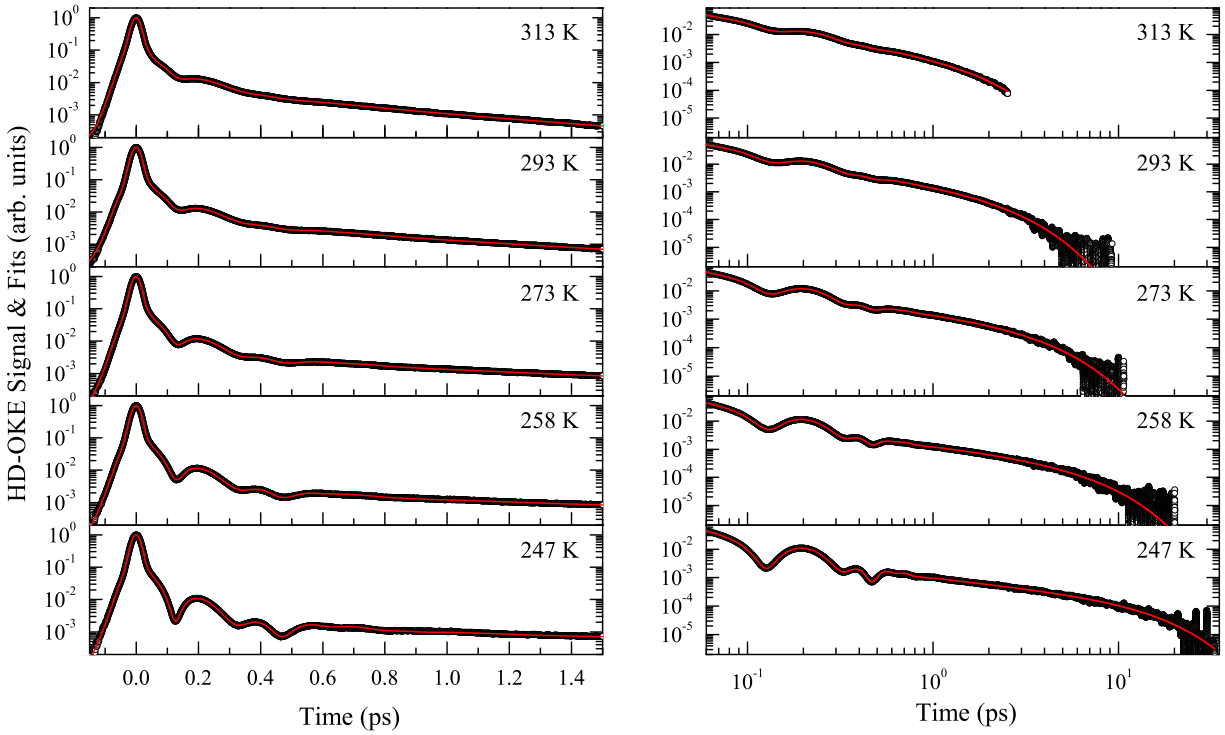

FIG. 3. The complex vibrational dynamics taking place in the sub-picosecond time scale is correctly reproduced by the numerical solution of the SMC model. The SMC model enables a very good fit of the slow relaxation decays, corresponding to the stretched exponential function. Also at intermediate delay times, where the vibrational dynamics merge into the relaxation processes, the decay curve is correctly described by the SMC equations. We report the SMC fits (red line) of the HD-OKE data (circle) for five temperatures. In the left panel the short time window is shown in a log-linear plots, in the right panel the whole time window is shown in a log-log plots.

trum $S_{DLS}(\omega)$ measured in the depolarized light scattering (DLS) experiments: the imaginary part of $\tilde{R}(\omega)$ is proportional to $S_{DLS}(\omega)$ corrected for the Bose factor, i.e $Im[\tilde{R}(\omega)] \propto S_{DLS}(\omega)/[n(\omega)+1]$ [28, 40]. Our results then can be directly compared to the DLS, Rayleigh and Raman, found in the literature. The imaginary part of the Fourier transform of the HD-OKE data and the calculated response are reported in Fig.4. The experimental spectra clearly show the characteristic vibrational features of liquid water: the two broad bands around 50 and 200 cm^{-1}, and the low frequency wing. This wing corresponds to the slow decay of the OKE signal measured in the time domain; as discussed in our previous work [29], it is attributed to structural relaxation.

The other two bands are generally attributed to translational intermolecular modes (i.e. the oscillating dynamics of water molecules around their instantaneous center of mass) hindered by the first neighbour molecular cage [37, 45, 46]. In the liquid phase they are largely affected by the hydrogen bonds. A comparison with the calculated vibrational density-of-states reported in ref. [45] suggests specific assignment of the 50 and the 200 cm^{-1} bands. The first one is dominated by the transverse translational motion, while the second has essentially longitudinal character [45]. The physical interpretation is that the two intermolecular vibrations are mainly involve "bending" and "stretching" distortion of the hydrogen bonds, respectively [23]. This picture even if intuitively useful, is clearly oversimplified: it doesn't take into account the coupling of the two vibrations imposed by the complex hydrogen bond network present in the liquid water. The presence of two different local structures, the one corresponding to highly tetrahedral intermolecular structures, and that consisting of strongly distorted network, as well as their continuous reorganization induced by the structural relaxation processes, are expected to strongly affect the vibrational dynamics. The SMC fit enables to disentangle the vibrational modes contributing to this dynamics and to point out their coupling to the structural relaxation processes. The bending mode at about 50 cm^{-1} is described by a single correlator (magenta line in Fig.4) that turns out to be decoupled from the structural relaxation (the peak close to 0 frequency). In contrast, the stretching mode, around 200 cm^{-1}, needs two correlators to be properly reproduced. One correlator, peaked at about 180 cm^{-1} (blue line), shows an almost temperature independent peak amplitude and a large spectral component extending to very low frequency, indicative of strong coupling to the structural dynamics. The other correlator, peaked at about 220 cm^{-1} (green line), appears to be substantially uncoupled to the structural dynamics; its amplitude increases with decreasing temperature. Our HD-OKE measurement represents the first clear experimental determination of this feature, even if it was inferred in a previous Raman study [21].

A comparison between these results and the recent debate on the nature of water anomalies is due. Our data and analysis show the presence of two distinct modes responsible for the part of the water spectrum normally attributed to the inter-molecular stretching vibrations. Raman spectra of low and high-density amorphous ice (LDA and HDA) in this frequency region differ from that of liquid water [47]. LDA has a broad peak centred at higher frequency, about 215 cm^{-1}, HDA shows an even broader peak centered at about 185 cm^{-1}

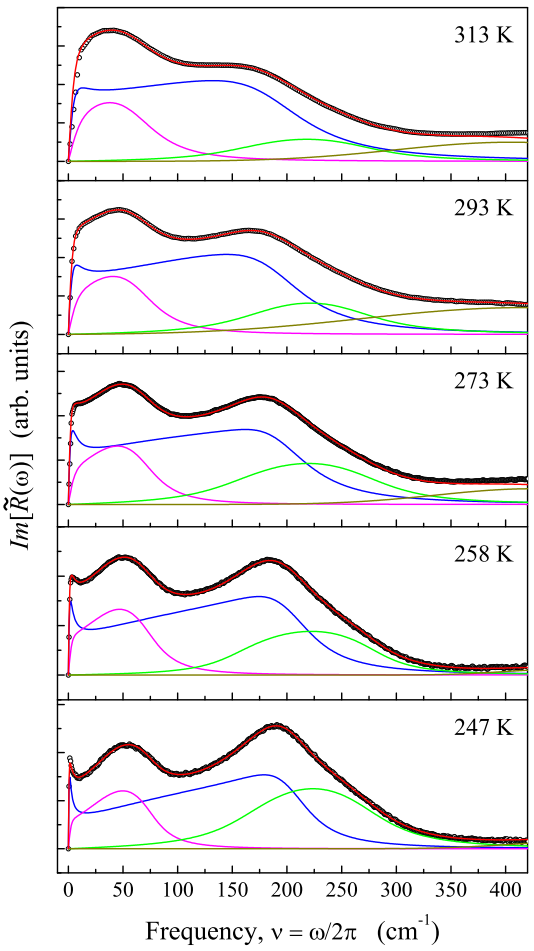

FIG. 4. The Fourier transform of the time-dependent HD-OKE response, $\tilde{R}(\omega)$, can be directly compared to the frequency-dependent spectrum measured in the DLS experiments, $S_{DLS}(\omega)$. The imaginary part of the Fourier transform of the HD-OKE data ($\circ$), after that the contribution of the instrumental function has been removed by de-convolution (see supplementary information) and of SMC fits (red line) at 247-258-273-313 K are reported in the frequency scale, $\nu = \omega/2\pi$. The SMC model allows to disentangle the dynamical features that generate the response function used in the fit. The contributes of the three slave correlators are reported in the figure as magenta-blu-green lines. The contribution of the very high frequency components ($\nu > 400$ cm^{-1}) of the response is included in the fit by means of a simple damped harmonic oscillator. This does not affect the response function in the lower frequency range, where the dynamics relevant to our investigation takes place.

(see for example fig.1 in ref. [47]) whereas the crystalline ice phases typically have a narrow peak at 230-240 cm^{-1}. This suggests that the modes observed in our experimental investigations can be associated with two fluctuating water species with different local structures; a low-density form (LD) characterized by tetrahedral network and four-coordinated molecules similar to the LDA structure, and a high-density (HD) form characterized by closely packed aggregates with lower coordination and high network distortions. The mode at 220 cm^{-1} can be attributed to the LD form and the mode at 180 cm^{-1} to the HD one. The present data strongly support the existence of the LD and HD water species. Nevertheless, as the observed water dynamic is measured at temperature/pressure relatively far from the supposed LLCP, some ambiguity remains about the nature of the critical phenomena taking place into the supercooled phase. The spectroscopic features attributed to the LD and HD forms could be attributed either to the coexistence of two extended liquid phases leading to the liquid-liquid phase transition [1, 3, 5], or to the continuous transition from a normal, unstructured liquid to a tetrahedrally structured liquid [9].

Our new experimental data and analysis clearly show the presence of the high-frequency satellite mode contributing to the intermolecular stretching band of water, whose amplitude increases sharply when the temperature goes deep in the supercooled phase. The nature of this mode, peaked at 220 cm^{-1}, appears clearly different from that of the nearby mode at 180 cm^{-1}. In fact, the former is strongly temperature dependent and only weakly coupled to the structural relaxation processes, while the latter is almost temperature independent and strongly coupled to structural rearrangements. The surprising similarities with the spectra of LDA and HDA glass forms with that of the two high frequency distinct modes, reported in this work, suggest attributing them to the LD and HD water structures, respectively. The LD water forms are expected to consist of aggregates of a small number of molecules; being mostly localized in space (at least in the temperature range investigated), their dynamics show negligible coupling with the structural relaxation. The number/lifetime of the LD species must increase with decreasing temperature in order to account for the amplitude increase of the corresponding correlator revealed by our analysis. On the other hand, the vibrational dynamics of the fraction of HD water appears dominated by the bare caging effect that merges into the structural relaxation, a behaviour typical of fragile glass-former liquids.

ACKNOWLEDGMENTS

The research has been performed at LENS. This work was supported by REGIONE TOSCANA POR-CRO-FSE 2007-2013 by EC COST Action MP0902-COINAPO and by PRIN 2010/2011 N.2010ERFKXL. We would like to thank A. Marcelli for helpful discussion. We acknowledge M. De Pas, A. Montori and M. Giuntini for providing their continuous assistance in the set-up of the electronics. R. Ballerini and A. Hajeb for the accurate mechanical realizations.

Appendix A: Supplemenraty Information

1. Experimental features

Supercooling bulk water is not an easy task because of crystallization. Temperatures as low as 20 degrees below melting can be achieved only with particularly pure sample and using specific attention for the cooling procedure. In our work we performed the measurements on bi-distilled water prepared by the Angelini company in a sealed vial of cylindrical shape, which enables us to reach a temperature as low as 247 K. The sample temperature is controlled with a stability of 0.1 K by means of a home-made cryostat. The vial is inserted into a parallelepiped-shaped aluminium holder, with a central cylindrical housing whose diameter is close to that of the vial. Two fused silica windows on opposite sides of the aluminium holder allow the beams to cross the sample. A thin film of glycerol between the vial and the housing assures an efficient heat transfer. The holder is fixed to the cold plate of a Peltier cooler and the temperature is controlled by a platinum thermoresistance in thermal contact with the holder itself.

A self-mode-locked Ti:sapphire laser (by Femtolasers, mod. Fusion: 25 fs pulse duration, 3 nJ pulse energy, 77.47 MHz repetition rate, 800 nm wavelength) was used for the experiments. Water is a liquid that has a very low OKE signal due to its nearly isotropic molecular polarizability. Our set-up enables measurement of the fast vibrational dynamics and the slow structural relaxation in a single experiment, with high signal-to-noise ratio. The delay time was scanned by means of the continuous motion of a translation stage, whose absolute position was controlled by a linear encoder [48]. This method reduces the acquisition time substantially, while improving the signal statistics. We adopted a peculiar

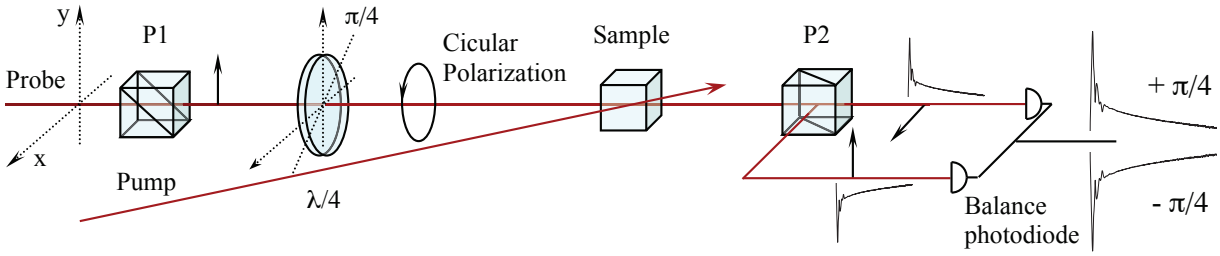

FIG. 5. Heterodyne detection scheme of OKE esperiment.

configuration for the heterodyne detection [31, 49], with circularly polarized probe beam and differential acquisition of two opposite-phase signals on a balanced double photodiode. With reference to Fig.5, a quarter wave-plate placed between the two polarizers produces a circularly polarized probe field. Two signals, corresponding to the horizontal and vertical linear polarizations generated by polarizer P2 and having a opposite sign, are sent to the balanced photodiode detector. Thus the measured OKE signal is automatically heterodyned and free from possible spurious signals. A further improvement of the data quality was obtained by subtracting the two HD-OKE measurements, corresponding at left and right circular polarizations of the probe field. This procedure removes from the signal the spurious dichroic contributions coming from possible misalignment of the wave-plate.

2. HD-OKE signal

The signal measured in an HD-OKE experiment is [50, 51]:

$$S(\tau) = \int dt |E_{pr}(t-\tau)|^2 \int dt' R(t-t') |E_{ex}(t')|^2 \tag{A1}$$

where E_{pr} and E_{ex} are the probing and exciting laser fields, respectively; $R(t)$ is the material response function. Since we are performing a non-resonant OKE experiment, the Born-Oppenheimer approximation applies and the *response function* can be cast in the form [51–53]:

$$R(t) = \gamma\delta(t) + R_n(t) \tag{A2}$$

with γ representing the instantaneous electronic response and $R_n(t)$ the nuclear response. The latter can be rewritten as

$$R_n(t) = -\frac{\theta(t)}{KT}\frac{\partial}{\partial t}\Phi_{\chi\chi} \tag{A3}$$

with $\Phi_{\chi\chi} = \langle \chi_{xy}(t)\chi_{xy}(0)\rangle$ where $\chi_{xy}(t)$ is the off-diagonal element of the collective electronic polarizability tensor. The Fourier transform of time-dependent response, $\tilde{R}(\omega)$, can be directly connected with the signal $S_{DLS}(\omega)$ measured in the depolarized light scattering (DLS) experiments. In fact, the imaginary part $Im[\tilde{R}(\omega)]$ is proportional to the DLS signal measured in forward configuration, i.e $Im[\tilde{R}(\omega)] \propto S_{DLS}(\omega)/[n(\omega)+1]$ [51].

In order to fit the OKE data we simulated the measured signal using the following expression [38, 54]:

$$S(t) = \int \left[\gamma\delta(t-t') + R_n(t-t')\right] G(t')dt' \tag{A4}$$

where $G(t)$ is the instrumental function accounting for the finite time resolution determined by the time width of the pump and probe pulses. Under specific conditions [38], $G(t)$ corresponds to the temporal autocorrelation of the laser pulse intensity. The experimental investigation of the instrumental function is the argument of the following paragraph.

3. The instrumental function measurement

An important experimental issue concerns the measurement of the real instrumental function $G(t)$, which is far from trivial. By definition, the instrumental function in a HD-OKE experiment is the signal measured in a system with response function $R(t) = \delta(t)$, as directly inferred from eq.A4. In practice, this condition can be fulfilled by choosing a sample with negligible nuclear response. In most of the papers published on this subject in recent years a fused silica plate has been used to this purpose, as its nuclear contribution is considered negligible.

In reality, silica presents a nuclear contribution, known to the glass physics community as "Boson Peak". Although this contribution is very weak, it prevents from measuring the real instrumental function. This is particularly relevant for water measurements, especially when investigating the fast dynamics. Alternatively, the instrumental function has been obtained by measuring the second harmonic autocorrelation of the laser pulse, or more simply by fitting the electronic contribution to the OKE signal with an analytic peak function (like Gaussian, hyperbolic secant, etc..).

In principle the second harmonic autocorrelation should be the best way to measure the instrumental function. It directly gives the temporal autocorrelation of the laser pulse intensity and, consequently, the temporal profile of $G(t)$. The procedure, however, implicates

some changes and adjustments in the OKE set-up: for instance, i) the insertion of a second harmonic crystal in place of the sample, with the consequent change of the pulse compression status, ii) the re-alignment of the beams and iii) the translation stage re-positioning in order to achieve the optimal temporal and spatial superposition of the pump and probe. All of these adjustment potentially modify the response function. Actually, any even small changes of the experimental conditions (e.g. a different beam alignment or a modified angle of superposition of the beams inside the sample) affect the instrumental function. Therefore, any method for obtaining the instrumental function that involves changes of the set-up is unsafe and can yield an incorrect time profile.

On the other hand, the accurate knowledge of the real instrumental function is mandatory to extract the true OKE response of water in the fast dynamics range. For this reasons we decided to extract the instrumental function by performing HD-OKE measurements in a reference sample. This procedure, differently from the second-harmonic approach, allows us to accurately preserve the experimental conditions used during the water measurements. As the reference sample we chose a plate of calcium fluoride (CaF_2). This a cubic ionic crystal which is optically isotropic and, in the frequency range probed in our experiment, has only one Raman active band at 322 cm^{-1}, due to the optical phonon T_{2g} symmetry. So the nuclear response of the reference sample is a simple and well known functional form. The calcium fluoride plate was dipped inside a water vial, identical to that used for water measurements, supported by the same sample holder.

The measurements of the instrumental function were done by just replacing the water vial with the water-CaF_2 vial, leaving the rest of the set-up unchanged. In the measurement we took care that the faces of the CaF_2 plate were perpendicular to the line bisecting the angle formed by pump and probe beams. The thickness of the CaF_2 plate, 3 mm, was enough to fully contain the probe and pump overlapping area, avoiding any spurious signal contribution by the outer water. We took a reference measurement for each set of water data. Maximum attention was taken to preserve the experimental conditions between the water and the reference measurement. Figure 6 reports a typical HD-OKE signal obtained in the CaF_2 reference sample: the signal shows a first peak, characterized by a very fast rise and fall, due to the electronic response, and a second oscillating contribution due to the nuclear response. This signal is the convolution of the instrumental function with the OKE response, see eq.A4, where the nuclear part is a single harmonic damped oscillator (DHO). The simplicity

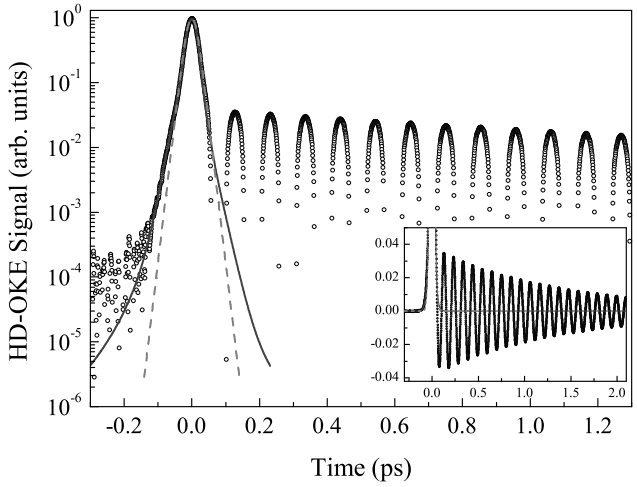

FIG. 6. HD-OKE signal of CaF_2 (circles). The continuous line is the instrumental function obtained with the fitting procedure described in the text. The nuclear response, R_n, is modelled as the time-derivative of a single damped oscillator and the instrumental function, G, is simulated as the sum of Gaussian, Lorentzian, and hyperbolic secant functions. The comparison with the fit of the instantaneous electronic part performed using just a single hyperbolic secant (dashed line) is reported too.

of this nuclear response function enables a reliable extraction of the instrumental function, $G(t)$, by means of an iterative fitting procedure (i.e. least square fitting of the HD-OKE data of the reference sample with the simulated signal according to eq.A4). We found that the instrumental function can not be reproduced by a single hyperbolic secant function, as often reported in the literature; a good fit requires the sum of several analytical functions, typically a combination of Gaussian, Lorentzian and/or hyperbolic secant functions. In fig. 6 we report the instrumental function obtained by the iterative fitting procedure (continuous line) and the one obtained by fitting the electronic peak with a simple hyperbolic secant function (dashed line). Apparently these two instrumental functions are very similar but the small differences cannot be neglected for an accurate investigation of water fast OKE response. This is mostly evident when the data are Fourier transformed to the frequency domain. In fact obtaining the imaginary part of the frequency dependent response from the time domain data involves the division by the Fourier transform of the instrumental function, i.e. $Im[\tilde{R}(\omega)] \propto Im\{FT\left[S(t)\right]/FT\left[G(t)\right]\}$. Fig. 7 shows the comparison between

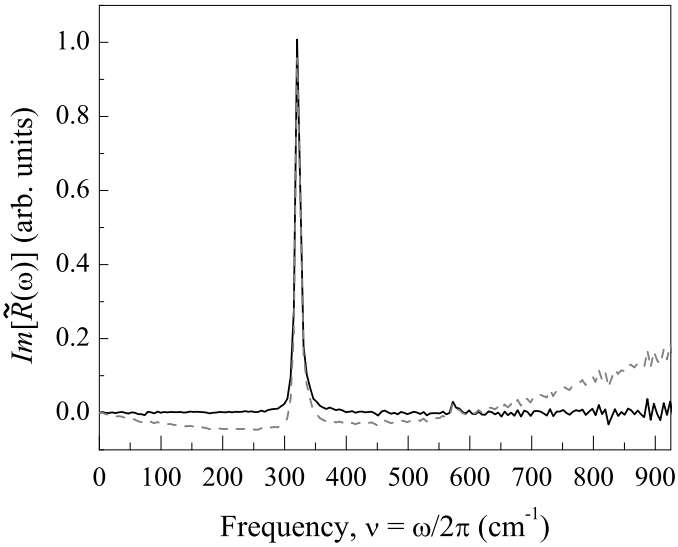

FIG. 7. Comparison between the calcium fluoride frequency dependent response calculated using the instrumental function obtained by the iterative fitting procedure (continuous line) and the one obtained by fitting the electronic peak with a hyperbolic secant function (dashed line). Only the knowledge of the real instrumental function allows measuring the correct response.

the response calculated using the instrumental function obtained by the iterative fitting procedure (continuous line) and the one obtained by simply fitting the electronic peak with a hyperbolic secant function (dashed line). We clearly see that only an accurate measurement of the real time domain instrumental function yields the correct response.

To our knowledge, this aspect of the OKE data analysis has never been addressed in such a quantitative way, and the present level of accuracy in analyzing the role the of the instrumental function in HD-OKE experiments is unprecedented in recent literature. In particular, we want to stress that the knowledge of the correct instrumental function is fundamental in order to extract the true OKE response, especially for the short delay time range. This is particularly critical for weak signals characterized by complex relaxation dynamics, as in the case of water.

4. Analysis by Schematic Mode-Coupling Model

The schematic mode-coupling (SMC) equations can be written as follows [44, 55–57]:

$$\ddot{\Phi}_m(t) + \eta_m \dot{\Phi}_m(t) + \Omega_m^2 \Phi_m(t) + \int K(t-t')\dot{\Phi}_m(t')dt' = 0 \tag{A5}$$

where the memory function is

$$K(t) = v_1 \Phi_m(t) + v_2 \Phi_m^2(t) \tag{A6}$$

The SMC model defines the memory by a series expansion on the *master correlator* itself Φ_m and provides in this way a closed form for the integro-differential equation A5. The SMC model identifies the master correlator as the density correlator $\Phi_m \propto \langle \rho(t)\rho(0) \rangle$. The dynamics of any other observable, A_i, linked to the density correlator dynamics (e.g. the molecular orientation, the target molecule dynamics, etc.) can be described by a similar differential equation [58]:

$$\ddot{\Phi}_i(t) + \eta_i \dot{\Phi}_i(t) + \Omega_i^2 \Phi_i(t) + \int m_i(t-t')\dot{\Phi}_i(t')dt' = 0 \tag{A7}$$

where

$$m_i(t) = v_i^s \Phi_m(t) \Phi_i(t) \tag{A8}$$

and $\Phi_i(t) \propto \langle A_i(t) A_i(0) \rangle$ is the *slave correlator*. The coupling between the slave and master dynamics is assured by the product between the slave and master correlators in the memory kernel m_i. Finally, the experimental observable can be expressed as sum of these slave correlators:

$$R^{SMC}(t) \propto \frac{\partial}{\partial t} \sum_i \Phi_i(t). \tag{A9}$$

According to eq.A9, in our analysis of the HD-OKE data we are decomposing the electronic polarizability correlator, $\Phi_{\chi\chi}$, into the sum of $\Phi_i(t)$ correlators. It is implicit that the individual slave correlators cannot be directly associated to specific physical variables. Each of these correlators in fact describes an "average collective mode" whose dynamics is described by the SMC equations. The vibrational and relaxation features and coupling processes are included in the SMC equations by definition. In this respect the present SMC equations A5-A9, represent a robust physical model able of describing a complex dynamics including vibrational and structural relaxations, implicitly accounting for their mutual coupling. Differently from other approaches, the method does not require any decoupling

or dynamic separation between the fast (vibrational) and the slow (relaxation) processes. Thus, once the temporal relaxation function of the master correlator is known, it can be used to calculate the relaxation of the slave correlators and, eventually, that of the OKE signal.

We found that the OKE data can be described in the entire temperature range by employing three slave correlators at most. In particular, the weight of the highest frequency contribution decreases monotonically with increasing temperature, becoming negligible at the two highest temperatures, where only two slave correlators are sufficient to reproduce the data. The parameters of the model are sixteen: the master equation parameters η_m, Ω_m, v_1 and v_2, the slave equations parameters η_i, Ω_i, v_i^s with $i = 1, 2, 3$ and finally the three amplitudes a_1, a_2, and a_3. The integro-differential equations A5 and A7 were solved numerically with a step by step second order Runge-Kutta algorithm. Preliminary series of fits provided a qualitative estimate of the temperature behavior of the parameters. In agreement with similar analyses reported in the literature [54–56, 59–62], in the subsequent step we forced some of the parameter either to assume fixed values or to follow simple temperature trends. In particular, we found that the frequency Ω_m and the vertex v_1 of the master oscillator are almost constant in the whole temperature range, and we locked their values to 66 cm^{-1} and 0.33, respectively. The second vertex v_2, instead, was found to increase almost linearly with decreasing temperature, and it was forced to obey the linear dependence $v_2 = 6 - 0.014T$. The friction parameter η_m and the remaining parameters of the slave oscillators were left free of varying. In figure 8 we show the temperature dependence of the slave frequencies Ω_i and the friction parameters η_m and η_i, and of the three vertices v_i^s. The temperature behavior of the fitting parameters is consistent with the results obtained by the previous studies in glass-former liquids [54–56, 59–62].

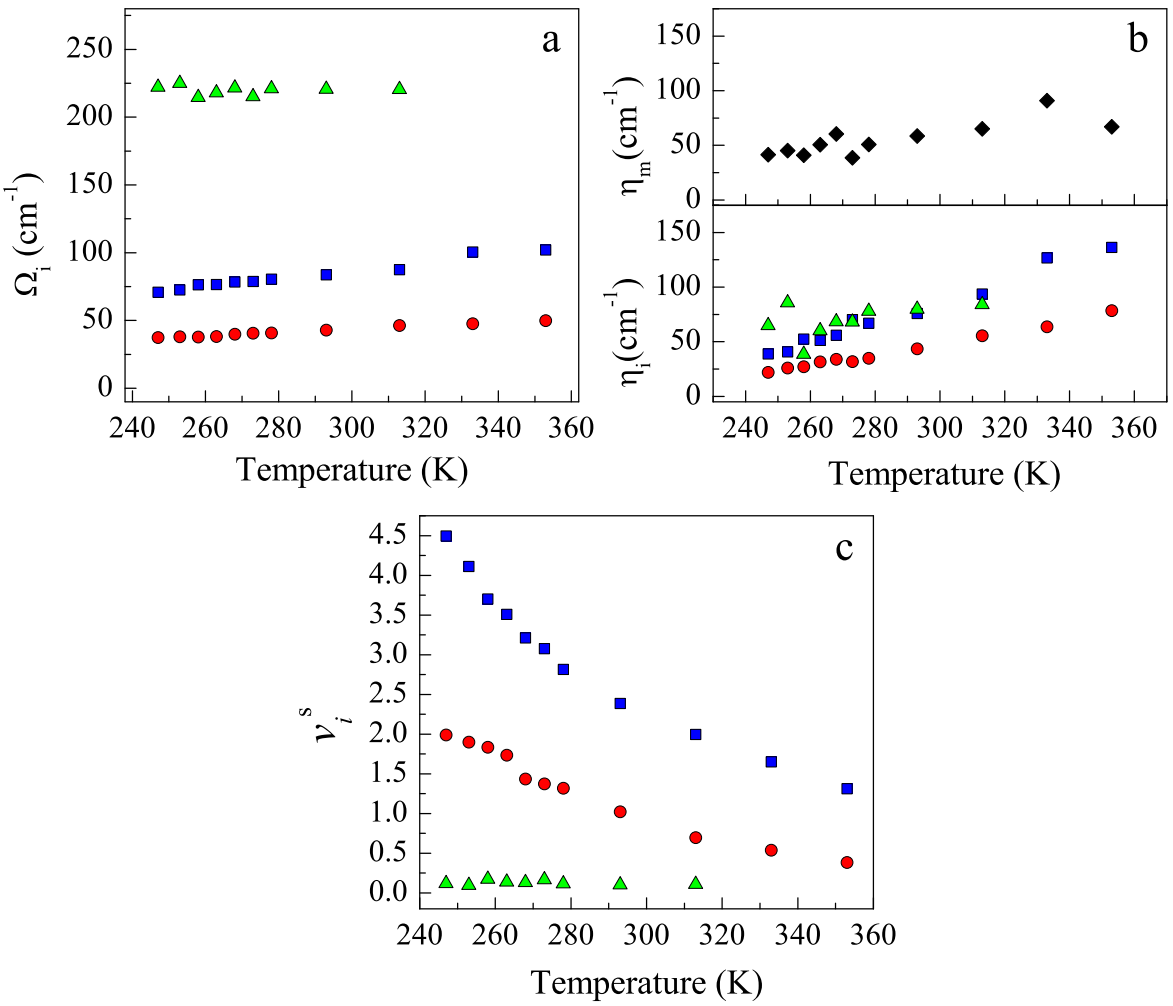

FIG. 8. Temperature behavior of the frequencies of the slave oscillators (circles, squares, and triangles refers to $i = 1$, 2, and 3, respectively) is reported in panel a). In panel b) we show the temperature behavior of the master and slave friction parameters (diamond refers to the master oscillator, circles, squares, and triangles refers to $i = 1$, 2, and 3, respectively). Temperature behavior of the vertices v_i^s (circles, squares, and triangles refers to $i = 1$, 2, and 3, respectively) are reported in panel c).

[1] O. Mishima and H.E. Stanley. The relationship between liquid, supercooled and glassy water. *Nature*, 396:329–335, 1998.

[2] P.G. Debenedetti and H. Eugene Stanley. Supercooled and glassy water. *Physics Today*, 56:40,

2003.

[3] Peter H. Poole, Francesco Sciortino, Ulrich Essmann, and H. Eugene Stanley. Phase behaviour of metastable water. *Nature*, 360:324–328, 1992.

[4] Yang Liu, Jeremy C. Palmer, Athanassios Z. Panagiotopoulos, and Pablo G. Debenedetti. Liquid-liquid transition in st2 water. *J. Chem. Phys.*, 137:214505, 2012.

[5] P.G. Debenedetti. Supercooled and glassy water. *J. Phys.: Cond. Matt.*, 15:R1669–R1726, 2003.

[6] A.K. Soper. Structural transformations in amorphous ice and supercooled water and their relevance to the phase diagram of water. *Mol. Phys.*, 106:2053–2076, 2008.

[7] C. A. Angell. Insights into phases of liquid water from study of its unusual glass-forming properties. *Science*, 319:582–587, 2008.

[8] A. Nilsoon and L.G.M. Pettersson. Perspective on the structure of liquid water. *Chemical Physics*, 389:1–34, 2011.

[9] Emily B. Moore and Valeria Molinero. Growing correlation length in supercooled water. *J. Chem. Phys.*, 130:244505, 2009.

[10] Emily B. Moore and Valeria Molinero. Structural transformation in supercooled water controls the crystallization rate of ice. *Nature*, 479:506, 2011.

[11] David T. Limmer and David Chandler. The putative liquid-liquid transition is a liquid-solid transition in atomistic models of water. *J. Chem. Phys.*, 135:134503, 2011.

[12] F. Sciortino, I. Saika-Voivod, and P. H. Poole. Study of the st2 model of water close to the liquid-liquid critical point. *Phys. Chem. Chem. Phys.*, 13:19759–19764, 2011.

[13] Peter H. Poole, Richard K. Bowles, Ivan Saika-Voivod, and Francesco Sciortino. Free energy surface of st2 water near the liquid-liquid phase transition. *J. Chem. Phys.*, 138:034505, 2013.

[14] T. A. Kesselring, G. Franzese, S. V. Buldyrev, H. J. Herrmann, and H. E. Stanley. Nanoscale dynamics of phase flipping in water near its hypothesized liquid-liquid critical point. *Scientific Reports*, 2:474, 2012.

[15] Paola Gallo and Francesco Sciortino. Ising universality class for the liquid-liquid critical point of a one component fluid: A finite-size scaling test. *Phys. Rev. Lett.*, 109:177801, 2012.

[16] A. Taschin, R. Cucini, P. Bartolini, and R. Torre. Temperature of maximum density of water in hydrophilic confinement measured by transient grating spectroscopy. *Europhys. Lett.*, 92:26005, 2010.

[17] R. Cucini, A. Taschin, P. Bartolini, and R. Torre. Acoustic, thermal and flow processes in a water filled nanoporous glass by time-resolved optical spectroscopy. *Journal of the Mechanics and Physics of Solids*, 58(9):1302–1317, 2010.

[18] P. Gallo, M. Rovere, and S.-H. Chen. Dynamic crossover in supercooled confined water: understanding bulk properties through confinement. *J. Phys. Chem. Lett.*, 1:729, 2010.

[19] R. Mancinelli, F. Bruni, and M.A. Ricci. Controversial evidence on the point of minimum density in deeply supercooled confined water. *J. Phys. Chem. Lett.*, 1:1277, 2010.

[20] Francesco Mallamace, Matteo Broccio, Carmelo Corsaro, AntonioFaraone, Domenico Majolino, Valentina Venuti, Li Liu, Chung-Yuan Mou, and Sow-Hsin Chen. Evidence of the existence of the low-density liquid phase in supercooled,confined water. *Proc. Nat. Acad. Sci. USA*, 104:424–428, 2007.

[21] S. Krishnamurthy, R. Bansil, and J. Wiafe-Akenten. Low-frequency raman spectrum of supercooled water. *J. Chem. Phys.*, 79:5863–5870, 1983.

[22] F. Aliotta, C. Vasi, G. Maisano, D. Majolino, F. Mallamace, and P. Migliardo. Role of h bond and cooperative effects in normal and supercooled water studied by anisotropic low frequency light scattering. *J. Chem. Phys.*, 84:4731, 1986.

[23] G.E. Walrafen, M.R. Fisher, M.S. Hokmabadi, and W.-H. Yang. Temperature depencence of the low- and high-frequency raman scattering from liquid water. *J. Chem. Phys.*, 85:6970, 1986.

[24] J. L. Rousset, E. Duval, and A. Boukenter. Dynamical structure of water: Low-frequency raman scattering from a disordered network and aggregates. *J. Chem. Phys.*, 92:2150, 1990.

[25] K. Mizoguchi, Y. Hori, and Y. Tominaga. Study on dynamical structure in water and heavy water by low-frequency raman spectroscopy. *J. Chem. Phys.*, 97:1961, 1992.

[26] A.P. Sokolov, J. Hurst, and D. Quitmann. Dynamics of supercooled water: Mode-coupling theory approach. *Phys. Rev. B*, 51:12865, 1995.

[27] Martin Chaplin. see referencee http://www.lsbu.ac.uk/water/.

[28] R. Torre. *Time-resolved spectroscopy of complex liquids, an experimental perspective*. New York: Springer, 2008.

[29] R. Torre, P. Bartolini, and R. Righini. Structural relaxation in supercooled water by time-resolved spectroscopy. *Nature*, 428:296–299, 2004.

[30] A. Taschin, P. Bartolini, R. Eramo, and R. Torre. Supercooled water relaxation dynamics

probed with heterodyne transient grating experiments. *Phys. Rev. E*, 74:031502, 2006.

[31] P. Bartolini, A. Taschin, R. Eramo, R. Righini, and R. Torre. Optical kerr effect measurement on supercooled water: the experimental perspective. *J. Phys.: Conf. Series*, 177:012009, 2009.

[32] A. Taschin, R. Cucini, P. Bartolini, and R. Torre. Does there exist an anomalous sound dispersion in supercooled water? *Philos. Mag.*, 91:1796–1800, 2011.

[33] E.W. Castner, Y.J. Chang, Y.C. Chu, and G.E. Walrafen. The intermolecular dynamics of liquid water. *J. Chem. Phys.*, 102:653–659, 1995.

[34] S. Palese, S. Mukamel, R.J.D. Miller, and W.T. Lotshaw. Interrogation of vibrational structure and line broadening of liquid water by raman-induced kerr effect measurements within multimode brownian oscillator model. *J. Phys. Chem.*, 100:10380, 1996.

[35] K. Winkler, J. Lindner, and P. Vohringer. Low-frequency depolarized raman-spectral density of liquid water from femtosecond optical kerr-effect measurements: Lineshape analysis of restricted translational modes. *Phys. Chem. Chem. Phys.*, 4:2144–2155, 2002.

[36] B. Ratajska-Gadomska, B. Biakowski, W. Gadomski, and Cz. Radzewicz. Ultrashort memory of the quasicrystalline order in water by optical Kerr effect spectroscopy. *Chem. Phys. Lett.*, 429:575–580, 2006.

[37] M.S. Skaf and M.T. Sonoda. Optical kerr effect in supercooled water. *Phys. Rev. Lett.*, 94:137802, 2005.

[38] D. Mc Morrow, W.T. Lotshaw, and G.A. Kenney-Wallace. Femtosecond optical kerr studies on the origin of the nonlinear responses in simple liquids. *IEEE J.Quantum Electron.*, QE-24:443–454, 1988.

[39] Yong-Xin Yan and Keith A. Nelson. Impulsive stimulated light scattering I: General theory. *J. Chem. Phys.*, 87:6240–6256, 1987.

[40] Yong-Xin Yan and Keith A. Nelson. Impulsive stimulated light scattering II: Comparison to frequency-domain light-scattering spectroscopy. *J. Chem. Phys.*, 87:6257, 1987.

[41] P. Bartolini, R. Ricci, R. Torre, R. Righini, and I. Santa. Diffusive and oscillatory dynamics of liquid iodobenzene measured by femtosecond optical kerr effect. *J. Chem. Phys.*, 110:8653–8662, 1999.

[42] R. Torre, P. Bartolini, and R. M. Pick. Time-resolved optical kerr effect in a fragile glass-forming liquids, salol. *Phys. Rev. E*, 57:1912–1920, 1998.

[43] R. Torre, P. Bartolini, R. Ricci, and R. M. Pick. Time-resolved optical kerr effect on a

fragile glass-forming liquid: Test of different mode coupling theory aspects. *Europhys. Lett.*, 52:324–329, 2000.

[44] W. Götze and L. Sjögren. Relaxation processes in supercooled liquids. *Rep. on Progress in Physics*, 55:241, 1992.

[45] A. DeSantis, A. Ercoli, and D. Rocca. Comment on an interpretation of the low-frequency spectrum of liquid water J. Chem. Phys. 118, 452 (2003). *J. Chem. Phys.*, 120:1657, 2004.

[46] J. A. Padró and J. Martí. Response to comment on an interpretation of the low-frequency spectrum of liquid water J. Chem. Phys. 118, 452 (2003). *J. Chem. Phys.*, 120:1659, 2004.

[47] Y. Suzuki, Y. Takasaki, Y. Tominaga, and O. Mishima. Low-frequency raman spectra of amorphous ices. *Chem. Phys. Lett.*, 319:81–84, 2000.

[48] P. Bartolini, A. Taschin, R. Eramo, and R. Torre. A real-time acquisition system for pump-probe spectroscopy. *Philos. Mag.*, 87:731–740, 2007.

[49] G. Giraud, C.M. Gordon, I.R. Dunkin, and K. Wynne. The effects of anion and cation substitution on the ultrafast solvent dynamics of ionic liquids: A time-resolved optical kerr-effect spectroscopic study. *J. Chem. Phys.*, 119:464–477, 2003.

[50] D. Prevosto, P. Bartolini, R. Torre, M. Ricci, A. Taschin, S. Capaccioli, M. Lucchesi, and P. Rolla. *Phys. Rev. E*, 66:011502, 2002.

[51] P. Bartolini, R. Eramo, A. Taschin, and R. Torre. *Time-resolved spectroscopy of complex liquids*, chapter Optical Kerr Effect Experiments on Complex Liquids, page 73. New York: Springer, 2008.

[52] R. W. Hellwarth. Third-order optical susceptibilities of liquids and solids. *Prog. Quant. Electr.*, 5:1–68, 1977.

[53] R. Torre, I. Santa, and R. Righini. Pre-transitional effects in the liquid-plastic transition of p-terphenyl. *Chem. Phys. Lett.*, 212:90–95, 1993.

[54] M. Ricci, S. Wiebel, P. Bartolini, A. Taschin, and R. Torre. Time-resolved optical kerr effect experiments on supercooled benzene and test of mode-coupling theory. *Philos. Mag.*, 84:1491–1498, 2004.

[55] W. Götze and T. Voigtmann. Universal and non-universal features of glassy relaxation in propylene carbonate. *Phys. Rev. E*, 61:4133, 2000.

[56] W. Götze and M. Sperl. Nearly-logarithmic decay of correlations in glass-forming liquids. *Phys. Rev. Lett.*, 92:105701, 2004.

[57] W. Götze. *Complex Dynamics of Glass-Forming Liquids, a mode-coupling theory.* Oxford: University Press, 2009.

[58] J. Bosse and U. Krieger. *J. Phys. C: Solid State Phys.*, 19:L609, 1987.

[59] C. Alba-Simionesco and M. Krauzman. *J. Chem. Phys.*, 102:6574, 1995.

[60] J. Wuttke, M. Ohl, M. Goldammer ana S. Roth, U. Schneider, P. Lunkenheimer, R. Kahn, B. Ruffl, R. Lechner, , and M. A. Berg. *Phys. Rev. E*, 61:2730, 2000.

[61] V. Krakoviack and C. Alba-Simionesco. *J. Chem. Phys.*, 117:2161, 2002.

[62] S. Wiebel and J. Wuttke. *New J. Phys.*, 4:56, 2002.